J Mol Model (2014) 20:2509
DOI 10.1007/s00894-014-2509-9

ORIGINAL PAPER

DFT study of the effect of solvent on the H-atom transfer involved in the scavenging of the free radicals $^{\bullet}HO_2$ and $^{\bullet}O_2^-$ by caffeic acid phenethyl ester and some of its derivatives

Olivier Holtomo · Mama Nsangou · Jean Jules Fifen · Ousmanou Motapon

Received: 29 July 2014 / Accepted: 20 October 2014 / Published online: 13 November 2014

Abstract H-atom transfer from caffeic acid phenethyl ester (CAPE), MBC (3-methyl-2-butenyl caffeate), BC (benzoic caffeate), P3HC (phenethyl-3-hydroxycinnamate), and P4HC (phenethyl-4-hydroxycinnamate) to the selected free radicals $^{\bullet}HO_2$ and $^{\bullet}O_2^-$ was studied. Such a transfer can proceed in three different ways: concerted proton-coupled electron transfer (CPCET), electron transfer followed by proton transfer (ET-PT), and proton transfer followed by electron transfer (PT-ET). The latter pathway is sometimes competitive with SPLET (sequential proton loss electron transfer) in polar media. Analyzing the thermodynamic descriptors of the reactions of CAPE and its derivatives with co-reactive species—in particular, the free energies of reactions, the activation barrier to the CPCET mechanism, and their rate constants—appears to be the most realistic method of investigating the H-atom transfers of interest. These analyses were performed via DFT calculations, which agree well with the data acquired from experimental studies (IC_{50}) and from CBS calculations. The CPCM solvation model was used throughout the work, while the SMD model—employed as a reference—was used only for CAPE. The main conclusion drawn from the analysis was that SPLET is the mechanism that governs the reaction of phenolic acids with $^{\bullet}HO_2$, while PT-ET governs the reaction of phenols with $^{\bullet}O_2^-$. In kinetic investigations of the CPCET process, the rate constant decreases as the solvent polarity increases, so the reaction velocity slows down.

Keywords CAPE · H-atom transfer · CPCM · SMD · Solvent effect · Rate constant · DFT · CBS

Electronic supplementary material The online version of this article (doi:10.1007/s00894-014-2509-9) contains supplementary material, which is available to authorized users.

O. Holtomo · O. Motapon
Laboratory of Fundamental Physics, Faculty of Science, University of Douala, DoualaP. O. Box 24157, Cameroon

O. Holtomo
Department of Physics, Faculty of Science, University of Bamenda, BamendaP. O. Box 39, Cameroon

M. Nsangou (✉)
Department of Physics, Higher Teacher's Training College, University of Maroua, MarouaP.O. Box 46, Cameroon
e-mail: mnsangou@yahoo.com

M. Nsangou · J. J. Fifen
Department of Physics, Faculty of Science, University of Ngaoundere, NgaoundereP.O. Box 454, Cameroon

Introduction

Phenolic compounds or polyphenols constitute one of the most numerous and ubiquitously distributed groups of plant secondary metabolites, with more than 8,000 phenolic structures currently known [1]. One group of phenolic compounds—phenolic acids (PhAs) and their derivatives—are widely present in plants (vegetables, fruits, grains, and spices), and several functions are attributed to them [2, 3]. For example, PhAs may contribute to the dark color, bitter taste, and objectionable flavor of some fruits, leaves, and seeds. They have been considered possible influences on the toxicological, nutritional, sensory, and antioxidant properties of foods [2, 3].

Caffeic acid phenethyl ester (CAPE) is a phenolic acid isolated from propolis (a substance that honeybees use to reduce entrance size and to seal holes in their hives [4–8]). This molecule is known to have antioxidative [2, 3], antiatherosclerotic [6], antiviral [9], antibacterial [10], anti-inflammatory [11, 12], and immunostimulatory [13] properties. Sud'ina et al. [14] studied the inhibitory effect of CAPE on the superoxide generated by stimulated neutrophiles. A crystallographic analysis of CAPE was performed by Son et al. [5]. Recently, Sestili et al. [7] studied the effects of some polyphenols, including CAPE and some of its derivatives, on

damage to DNA. Many studies [14–25] have been carried out to search for and to develop antioxidants of natural origin. The potential use of CAPE and its derivatives as natural compounds has drawn substantial attention because of their occurrence in nature.

Free radicals that can be scavenged by CAPE or its derivatives are produced by exogenous (ionizing radiations, UV light, or pollution) or endogenous (e.g., the production of $^{\bullet}O_2^-$) processes. Different cascades of events, such as the oxidation of lipids in cell membranes, produce a huge variety of free-radical species. In 1954 Gershman, Gilbert, and Fridovich suggested that the superoxide anion radical ($^{\bullet}O_2^-$) is responsible for oxygen toxicity. However, although it is highly reactive, it was found to be unreactive in aprotic environments and towards amino acids and lipids [26]. Michelson et al. [27] showed in 1977 that these species are present in biological cells at the level of about 10^{-11} mol/L, and that this level is kept essentially constant by superoxide dismutase (SOD). Hydroperoxyl $^{\bullet}HO_2$ is the protonated form of $^{\bullet}O_2^-$ (pK_a=4.88). It is a much stronger oxidant than $^{\bullet}O_2^-$, and was initially thought to be responsible for the toxic effects of oxygen and for cell membrane damage by Liochev and Fridovich in 2001 [28]. $^{\bullet}HO_2$ has a relatively long lifetime and so can diffuse to neighboring structures. At the physiological pH of 7.4, about 1 % of superoxide exists in its protonated form [26]. Imbalances of these free radicals in the physiological environment can damage DNA, proteins, and lipids. All of this information led us to focus on the radicals $^{\bullet}HO_2$ and $^{\bullet}O_2^-$ in our study.

The structure–activity relationships of the antioxidant capacities of CAPE and its derivatives have been established theoretically and rationalized on the basis of quantum-chemical studies [8]. The calculated thermodynamic descriptors for these molecules, such as their O–H bond dissociation enthalpies (BDEs), proton affinities (PAs), ionization potentials (IPs), and π-electron conjugation, fit perfectly with their free-radical scavenging activities, particularly when these parameters are calculated at the DFT (density functional theory) level using a hybrid functional (B3LYP). Those calculations confirm (i) the important role of the $-O_3H_3$ group of CAPE and its derivatives, (ii) the important role of the double bond and the catechol moiety, and (iii) the significant effect of the solvent on all of the parameters that influence the antioxidant activities of the molecules (see Fig. 1).

These thermodynamic parameters are now utilized to predict the capacity of polyphenols to act as antioxidants in vitro (outside of the organism). However, the thermodynamic approach cannot accurately predict free-radical scavenging activities in organisms. To be a satisfactory antioxidant, a polyphenol must react by H-atom transfer faster than at least one of the reactions of the free-radical production cascades, so an accurate description of the kinetics of H-atom transfer between polyphenols and free radicals is a crucial step towards predicting their biological activities in vivo (in the organism). The experimental exploration of antioxidant kinetics is rather too delicate to be systematically performed for a large series of compounds under various conditions (different media) [15–17]. Quantum chemistry is therefore a useful way to logically evaluate kinetic aspects in which the rate constants are directly calculated. Nevertheless, to achieve sufficient accuracy, the theoretical methodology applied must be carefully chosen. A suitable qualitative description would prove useful to establish structure–activity relationships in terms of kinetics. An accurate quantitative description would allow antioxidant activities to be predicted in vivo.

The antioxidants PhOH are powerful free-radical scavengers. During this scavenging, H-atom transfer (HAT) occurs from their –OH groups to the free radicals ($R^{\bullet}$). This H-atom transfer can proceed through the following pathways:

(i) The HAT or CPCET mechanism:

$$PhOH + R^{\bullet} \rightarrow PhO^{\bullet} + RH \qquad (A) \tag{1}$$

(ii) The ET-PT mechanism:

$$PhOH + R^{\bullet} \rightarrow PhOH^{\bullet+} + R^- \quad (B^1) \quad \rightarrow PhO^{\bullet} + RH \quad (B^2) \tag{2}$$

(iii) The PT-ET mechanism:

$$PhOH + R^{\bullet} \rightarrow PhO^- + RH^{\bullet+} \quad (\Gamma^1) \quad \rightarrow PhO^{\bullet} + RH \quad (\Gamma^2) \tag{3}$$

(iv) The SPLET mechanism:

$$\begin{aligned} PhOH &\rightarrow PhO^- + H^+ && (\Delta^1) \\ PhO^- + R^{\bullet} &\rightarrow PhO^{\bullet} + R^- && (\Delta^2) \\ R^- + H^+ &\rightarrow R\ H && (\Delta^3) \end{aligned} \tag{4}$$

It is noticeable that the two first pathways start with PhOH + $R^{\bullet}$ and end with $PhO^{\bullet}$ + RH. ET-PT is a two-step mechanism involving an electron transfer (B^1) followed by a proton release (B^2). PT is so fast that ET-PT can be considered a HAT process; this was proven in the literature [15–17]. PT-ET is the reverse mechanism with respect to the ET-PT mechanism; it is described by the two steps Γ^1 and Γ^2. This pathway is, according to the literature [18–21], likely to occur in the presence of neutral free radicals, so it can happen via the SPLET mechanism, which involves proton loss (Δ^1) followed by electron transfer from the polyphenol anion (Δ^2). SPLET is favored when the anion (PhO^-) is stable enough to allow electron transfer before reprotonation. All of those pathways

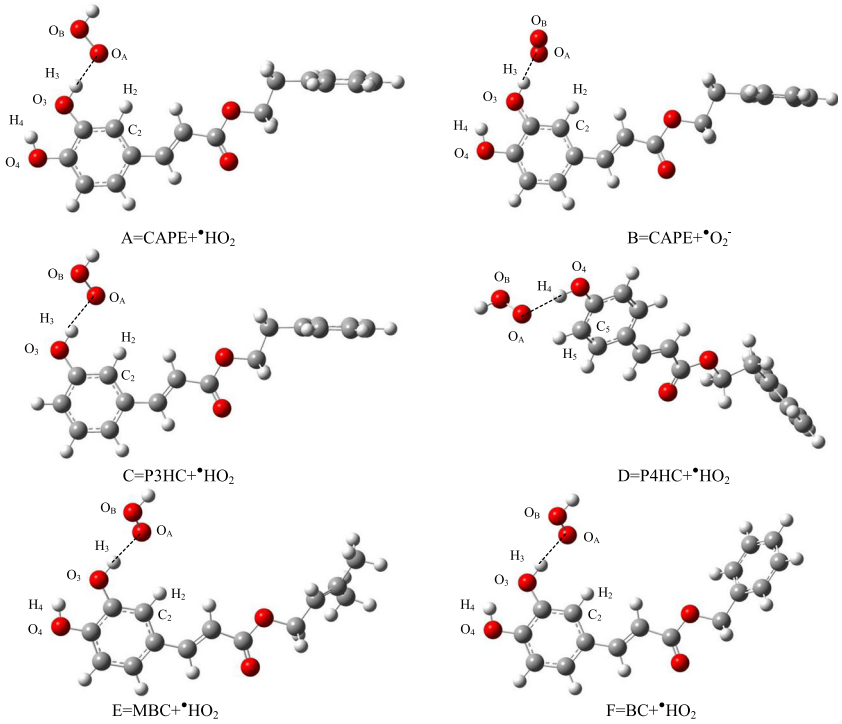

Fig. 1 Equilibrium geometries of the supermolecules formed in reactions A, B, C, D, E, and F

are solvent dependent [23–25], and they may co-exist in some chemical or biological systems [29].

To characterize each pathway, the reaction free energy was evaluated as the free energy in each reaction A, B^1, B^2, Γ^1, Γ^2, Δ^1, and Δ^2:

$$\Delta_f G^\circ(A) = \Delta_f G^\circ(PhO^\bullet) + \Delta_f G^\circ(RH) - \Delta_f G^\circ(PhOH) - \Delta_f G^\circ(R^\bullet) \quad (5)$$

$$\Delta_f G^\circ(B^1) = \Delta_f G^\circ(PhOH^{\bullet+}) + \Delta_f G^\circ(R^-) - \Delta_f G^\circ(PhOH) - \Delta_f G^\circ(R^\bullet) \quad (6)$$

$$\Delta_f G^\circ(B^2) = \Delta_f G^\circ(PhO^\bullet) + \Delta_f G^\circ(RH) - \Delta_f G^\circ(PhOH^{\bullet+}) - \Delta_f G^\circ(R^-) \quad (7)$$

$$\Delta_f G^\circ(\Gamma^1) = \Delta_f G^\circ(PhO^-) + \Delta_f G^\circ(RH^+) - \Delta_f G^\circ(PhOH) - \Delta_f G^\circ(R^\bullet) \quad (8)$$

$$\Delta_f G^\circ(\Gamma^2) = \Delta_f G^\circ(PhO^\bullet) + \Delta_f G^\circ(RH) - \Delta_f G^\circ(PhO^-) - \Delta_f G^\circ(RH^+) \quad (9)$$

$$\Delta_f G^\circ(\Delta^1) = \Delta_f G^\circ(PhO^-) + \Delta_f G^\circ(H^+) - \Delta_f G^\circ(PhOH) \quad (10)$$

$$\Delta_f G^\circ(\Delta^2) = \Delta_f G^\circ(PhO^\bullet) + \Delta_f G^\circ(R^-) - \Delta_f G^\circ(PhO^-) - \Delta_f G^\circ(R^\bullet) \quad (11)$$

It is known from the literature [8, 24, 25, 30] that, in the absence of any co-reactive species, the homolytic hydrogen atom transfer (HHAT) pathway is favored in nonpolar solvents. This pathway is dictated by the bond dissociation enthalpy (BDE). In strongly polar solvents, the pathway favored is sequential electron transfer followed by proton transfer (SET-PT), which is governed by the ionization potential (IP). In addition, the four mechanisms (Eqs. 1–4) have the same reaction free-energy balance because the reactants and products are the same ($\Delta G^{CPCET} = \Delta G^{ET\text{-}PT} = \Delta G^{PT\text{-}ET} = \Delta G^{SPLET}$), so the competition between the different mechanisms is described by either the reaction free energy or the kinetics of the rate limiting step of each mechanism (atom transfer for CPCET, proton transfer for PT-ET, and electron transfer for both ET-PT and SPLET).

In the work reported in the present paper, we computed the reaction free energy ΔG of the limiting step of each H-transfer mechanism (CPCET, ET-PT, PT-ET, and SPLET) employed by CAPE and four of its derivatives (MBC, BC, P3HC, and P4HC) in the presence of neutral ROS ($HO_2^\bullet$), taking into account the results for the kinetics of the CPCET process for each molecular system with the radical $^\bullet HO_2$, in order to evaluate the activation energy and corresponding rate constant. The same investigation was performed for the reaction free energies of the CPCET and PT-ET processes in the presence of ionic ROS ($^\bullet O_2^-$). Finally, the preferred mechanism involved in the H-atom transfer of each molecule in the family of antioxidants listed above was determinied. Since the damage caused by free radicals occurs in the physiological environment, these studies were carried out in a vacuum as well as in nonpolar and polar solvents (cyclohexane, benzene, dichloromethane, methanol, and water).

Computational methods

DFT, basis sets, and solvation method description

CAPE and its derivatives (PhOH), as well as their corresponding radicals ($PhO^\bullet$), cations ($PhOH^{\bullet+}$), and anions (PhO^-),

were found to be accurately described by DFT calculations [8]. The B3LYP functional permits a particularly accurate evaluation of the thermodynamics of the reactions between polyphenols and free radicals [8].

Computations were carried out using density functional theory (DFT) implemented in the Gaussian 03W computational package [31]. The choice of DFT was supported by the excellent compromise observed between the computational time and the description of the electronic correlation. The B3LYP hybrid functional was used throughout the computations. This functional consists of Becke's three-parameter exact exchange functional (B3) [32] combined with the nonlocal gradient-corrected correlation functional (due to Lee–Yang–Parr, LYP) [33]. The split valence double zeta basis sets 6-31G(d,p) and 6-31+G(d,p) were used throughout the computation process. These basis sets consist of the standard Gaussian basis 6-31G of Pople et al. [34–39] supplemented by two sets of polarization functions (a set of *d* functions acting on heavy atoms and a set of *p* functions acting on light atoms) [40].

Geometry optimizations (B3LYP/6-31G(d,p)), followed by frequency (B3LYP/6-31+G(d,p)) calculations, were carried out without constraints up to convergence (largest component of the nuclear gradient was equal to 10^{-6} a.u./bohr, and the change in total energy was less than 10^{-7} a.u.).

All of these calculations were undertaken in vacuum and in five solvents. Solvation was taken into account in a hybrid manner, considering some explicit interactions between the particle to be transferred (during the scavenging mechanism) and a solvent molecule. The rest of the solvent was treated implicitly using the conductor-like polarized continuum model (CPCM); the solute was assumed to be placed into a cavity created in a dielectric continuum. Due to the charge distribution of the solute, the continuum is polarized and creates an electric field inside the cavity that polarizes the solute in return. The solvents considered were cyclohexane, benzene, dichloromethane, methanol, and water. The universal solvation model (SMD) based on the solute's electron density and on a continuum model of the solvent [41] was also used for the calculations of CAPE in the presence of benzene or water. This extra calculation was done due to a lack of experimental data and also because the SMD method has been proven elsewhere to be more realistic than the CPCM [42], so it could be used as a reference. Since the SMD method is not available in the Gaussian 03 package, these computations were done with the Gaussian 09 computational package.

CBS (complete basis set) calculations were performed for reactions involving $^{\bullet}O_2^-$ due to the fact that this method has been proven in previous calculations [43] to yield highly accurate free energies.

Rate constant computation

Rate constants were computed as a function of temperature *T* via the zero-order semi-classical transition state theory [44–46]. The rate constant for the canonical transition state theory (TST) is given by

$$k(T) = k_{\text{tunnel}}(T) \times k_{\text{TST}}(T), \tag{12}$$

where $k_{\text{TST}}(T)$ for the bimolecular reaction A+B→C+D is given by

$$k_{\text{TST}}(T) = \frac{\sigma}{\beta h}\frac{Q^*(T)}{Q_{\text{A}}(T)Q_{\text{B}}(T)}e^{-\beta\Delta V^{\neq}}. \tag{13}$$

Here, k_{TST} is the standard TST rate constant at temperature *T*, without tunneling correction. $\beta=1/k_{\text{B}}T$, $Q_{\text{A}}(T)$, $Q_{\text{B}}(T)$, and $Q^*(T)$ are, respectively, the partition functions (per unit volume) of the reactants A and B and the transition state at temperature *T*. *h* and k_{B} are, respectively, the Planck and Boltzmann constants. σ is the number of indistinguishable ways the reactants may approach the activated complex regions, as defined by Duncan et al. [45]. $\Delta V^{\neq}$ is the difference in zero points, including the potential energies of the reactants and the transition state (TS) structure. $k_{\text{tunnel}}(T)$ is the ground-state transmission coefficient at temperature *T*, which primarily accounts for the tunneling correction.

Canonical variational transition state theory

Canonical variational transition state theory (CVT) is an extension of TST. It minimizes the recrossing effects and provides a framework for a more accurate description of quantum tunneling effects. In this approximation, the transmission coefficient is a zero-order interpolated approximation [45, 47, 48]. By "zero order," the authors mean that no ab initio or DFT calculations at points other than the reactants, saddle points, and products are available. In addition, tunneling is assumed to occur along the minimum energy path (MEP), which is interpolated using an Eckart function [49]. Since it is unclear whether the highest point in the MEP corresponds to the highest free energy, the variational TST rate constant is defined as

$$k_{\text{CVT}}(T) = \min_s \left[\frac{\sigma}{\beta h}\frac{Q^*(T,s)}{Q_{\text{A}}(T)Q_{\text{B}}(T)}e^{-\beta\Delta V^{\neq}(s)}\right]. \tag{14}$$

Here, *s* denotes the distance from the generalized transition state along the MEP.

Quantum effects in this degree of freedom are included by multiplying the CVT rate constant by a ground-state transmission coefficient $k_{\text{tunnel}}(T)$.

Tunneling corrections

Usually, tunneling is considered only in the degree of freedom corresponding to the reaction coordinate. In our work, we

used the Wigner tunneling approximation for the transmission coefficient, which is known as the parabolic approximation [50, 51]:

$$k_{\text{tunnel}}(T) = 1 + \frac{1}{24}\left|\frac{\hbar\nu^*}{k_B T}\right|^2. \quad (15)$$

We have written a Fortran 90 program to calculate the rate constant; it uses the CVT approximation to interpolate the MEP using the Eckart function, and Wigner tunneling for the transmission coefficient.

Results and discussion

It was necessary to determine the antioxidant activities of CAPE and its derivatives in the presence of the free-radical oxygen species (ROS) $^{\bullet}HO_2$ or $^{\bullet}O_2^-$, which are neutral and ionic, respectively, as described in the "Introduction," in order to evaluate the thermodynamic balance of each reaction. These ROS can provide insight into the antioxidant activities when PhAs are in the presence of neutral ROS or in the presence of ionic ROS, as described in the literature [15–22]. Figure 1 shows CAPE in the presence of $^{\bullet}HO_2$ or in the presence of $^{\bullet}O_2^-$. It also shows each of MBC, BC, P3HC, and P4HC in the presence of $^{\bullet}HO_2$. It is worth mentioning that all of these geometries were derived at the B3LYP/6-31+G(d,p) level of theory.

Relaxed potential energy surfaces of reactions involving PhA and ROS

In order to find the transition state (TS), we performed simultaneous relaxed scans of the O_3–H_3 distance and the angle C_3–O_3–H_3. This was to localize the saddle point, which is the point at which the two curves generated by these scans meet. Figure 2 (see also Fig. 2.s in the "Electronic supplementary material," ESM) shows the relaxed potential energy surface (RPES) of CAPE in the presence of $^{\bullet}HO_2$ and the RPES of CAPE in the presence of $^{\bullet}O_2^-$. The RPESs of MBC, BC, P3HC, and P4HC in the presence of $^{\bullet}HO_2$ are also shown. It is clear that there is a potential barrier to the reaction involving the neutral radical $^{\bullet}HO_2$, but no barrier to the reaction involving the ionic radical $^{\bullet}O_2^-$. This conclusion is in good agreement with remarks made in the literature [2, 3, 22, 24, 25, 34–39]. Therefore, the scavenging of the hydroperoxide radical $^{\bullet}HO_2$ and the superoxide radical $^{\bullet}O_2^-$ by a PhA can be summarized by Eqs. 16 and 17, respectively:

$$PhOH + {}^{\bullet}HO_2 \rightarrow PhO^{\bullet}\ldots H^{\bullet}\ldots {}^{\bullet}HO_2 \rightarrow PhO^{\bullet} + H_2O_2 \quad (16)$$

$$PhOH + {}^{\bullet}O_2^- \rightarrow PhO^- + {}^{\bullet}HO_2 \quad (17)$$

For reactions of PhAs with neutral ROS ($^{\bullet}HO_2$), the transition state is the saddle point of the RPES. At that point, the O–H distance at site 3 is 1.40 Å for CAPE, MBC, and BC, while that at position 4 is 1.45 Å. The O–H distance at the TS for P3HC and P4HC is 1.50 Å. The angle C_3–O_3–H_3 is 109°, 114.1°, and 113.2°, respectively, for CAPE, MBC, and BC, whereas the angle C_4–O_4–H_4 is 123.1° at the TS for CAPE, MBC, and BC. Nevertheless, the angle C_3–O_3–H_3 is 113.2° for P3HC and the angle C_4–O_4–H_4 is 112.3° for P4HC at the TS.

Difference between the HHAT and CPCET mechanisms

The HHAT mechanism is a pure H-atom transfer in which the proton and the electron of the H atom are transferred to the same atomic orbital in the free radical. In contrast, the CPCET mechanism involves several molecular orbitals [17–20]. CPCET occurs in an H-bonding pre-reaction complex ($PhOH\cdots{}^{\bullet}HO_2$) in which proton transfer occurs along the H-

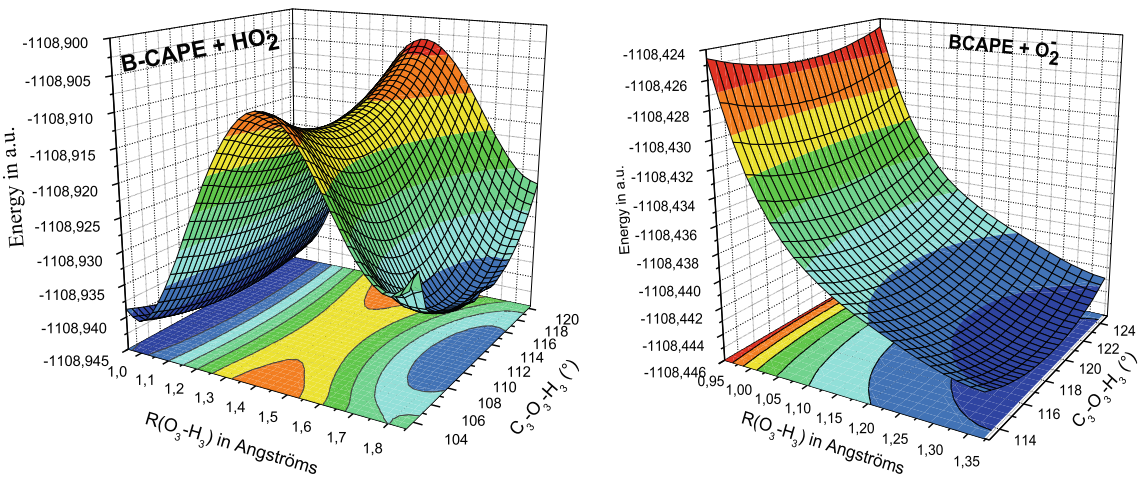

Fig. 2 3D-RPES for the reaction of B-CAPE with $^{\bullet}HO_2$ (*left*) and the 3D-RPES for the reaction of B-CAPE with $^{\bullet}O_2^-$ (*right*)

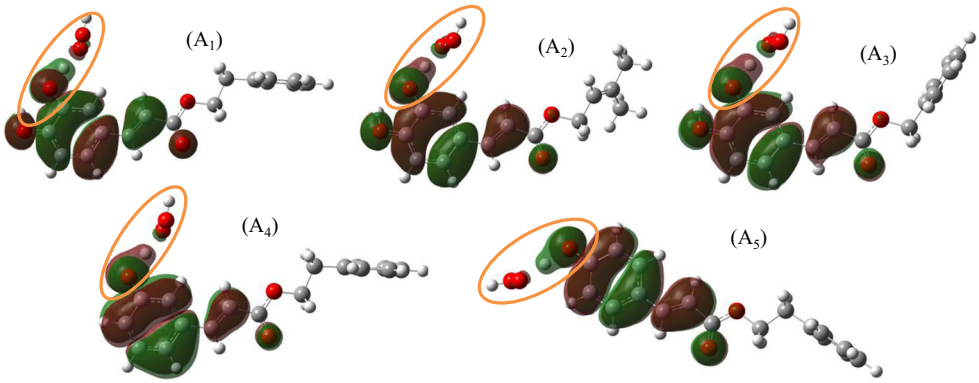

Fig. 3 SOMO distributions on the transition states associated with the reactions: *(A1)* B-CAPE with $^{\bullet}HO_2$, *(A2)* B-MBC with $^{\bullet}HO_2$, *(A3)* B-BC with $^{\bullet}HO_2$, *(A4)* B-P3HC with $^{\bullet}HO_2$, and *(A5)* B-P4HC with $^{\bullet}HO_2$

bond to one of the lone pairs of the O atom of the free radical. This transfer is coupled to the electron transfer that occurs from a lone pair of the antioxidant to the SOMO (singly occupied molecular orbital) of the free radical [2, 3, 17, 21, 22].

We will proceed as Mayer et al. [19] did in their work published in 2000, by analyzing the SOMO distribution on the transition state ($PhO^{\bullet}\cdots H^{\bullet}\cdots{}^{\bullet}HO_2$) and defining the mechanism that occurs (CPCET or HHAT). Figure 3 reveals that the orbitals on the donor–acceptor axis (the zone within the ellipse in each subfigure) are perpendicular, leading in this case to the CPCET mechanism. Therefore, the proton and the electron are transferred through two different orbitals from the studied molecules to $^{\bullet}HO_2$.

Scavenging of $^{\bullet}HO_2$ by CAPE and its derivatives

The free-radical scavenging action is governed by atom transfer (CPCET), proton transfer (PT-ET), or electron transfer (ET-PT and SPLET). These processes can proceed by overcoming the free-energy barrier or by tunneling along the reaction coordinate. In addition, as already pointed out in the "Introduction," a polyphenol must react by H-atom transfer faster than at least one of the reactions of the free-radical production cascades, so an accurate description of the kinetics of H-atom transfer between polyphenols and free radicals is required to be able to predict biological activities in vivo. This means that, at the very least, the rate constants of CPCET mechanism must be evaluated.

Atom transfer process: CPCET

As already described [2, 3, 15–17, 22], CPCET occurs when the pre-reaction complex $PhOH\cdots{}^{\bullet}HO_2$ is formed; H-bonds arise between the free radical and one of the −OH groups of the molecule under study (see Fig. 1). Thermodynamic and kinetic descriptions are necessary to understand this scavenging process.

(i) ***Thermodynamic investigations***

Table 2 displays the results for the free energies of reactions A_n, where n=3, 4 denotes the position of the −OH group on the ring of the molecule that reacts with $^{\bullet}HO_2$. The reported numerical values show that $\Delta G(A_3) < \Delta G(A_4)$ in a vacuum as well as in the solvents. Therefore, site 3 ($-O_3H_3$) remains favorable to scavenge free radicals, as noted recently [8]. The data also reveal that the free energy of reaction A_3 increases in the order

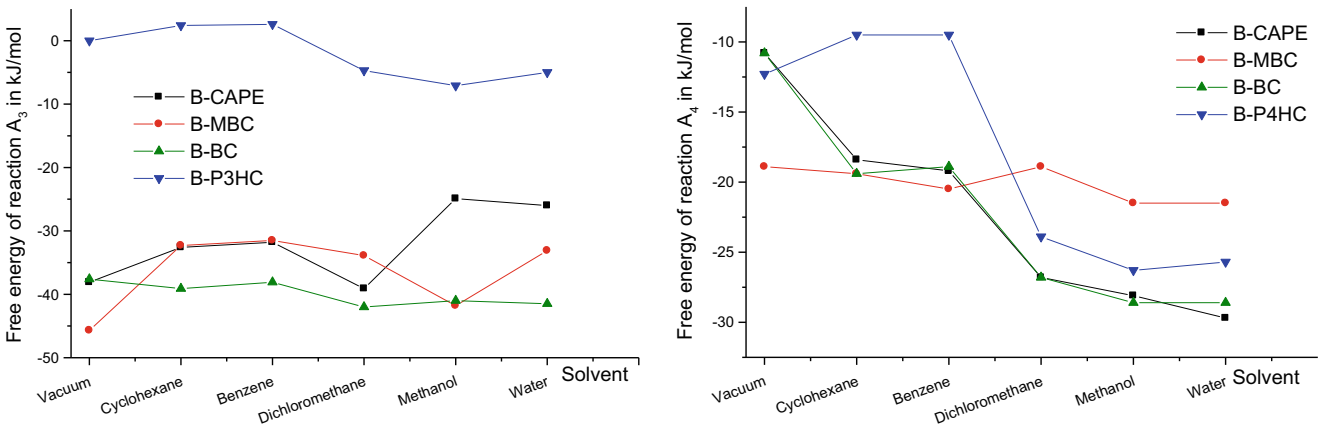

Fig. 4 Free energies of reactions A_3 (*left*) and A_4 (*right*) for B-CAPE, B-P4HC, P3HC, B-MBC, and B-BC in the presence of the radical $^{\bullet}HO_2$ in different media

Table 1 Parameters characterizing O–H cleavage in selected media: $k_{TST/ZCT}$ is the rate constant (in $Å^3\ mol^{-1}\ s^{-1}$), ΔE_a is the calculated activation energy (in kJ mol^{-1}), and ν^* is the imaginary frequency

System	Solvent	Related to the H_3 atom			Related to the H_4 atom		
		ΔE_a	ν^*	$k_{TST/ZCT}$	ΔE_a	ν^*	$k_{TST/ZCT}$
B-CAPE	Vacuum	207.5	−2399.7	7.37×10^{13}	264.9	−2523.9	2.15×10^{13}
	Benzene	210.5	−1522.8	8.33×10^{13}	–	–	–
	Water	225.1	−1595.5	2.57×10^{13}	–	–	–
B-MBC	Vacuum	202.9	−2442.5	8.21×10^{14}	253.6	−2524.9	1.08×10^{14}
	Benzene	208.0	−1745.4	6.77×10^{14}	–	–	–
	Water	236.4	−1679.4	1.09×10^{14}	–	–	–
B-BC	Vacuum	218.4	−2466.5	6.98×10^{14}	263.2	−2524.4	7.48×10^{13}
	Benzene	229.7	−1981.6	0.52×10^{13}	–	–	–
	Water	253.6	−1668.7	7.42×10^{13}	–	–	–
B-P3HC	Vacuum	255.6	−2482.9	9.23×10^{14}	–	–	–
B-P4HC	Vacuum	–	–	–	246.0	−2441.1	1.30×10^{15}

A_3(MBC) < A_3(CAPE) < A_3(BC) < A_3(P3HC), which agrees with the order found using the BDE_3 [8]. In solvents, BC has the lowest value of $\Delta G(A_3)$, so its antioxidant capacity is higher than those of the others. On the other hand, from site 4, we have A_4(MBC) < A_4(P4HC) < A_4(CAPE) ~ A_4(BC) in a vacuum, which again indicates that MBC is the strongest antioxidant. In strongly polar solvents (dichloromethane, methanol, and water), we have A_4(CAPE) ~ A_4(BC) < A_4(P4HC) < A_4(MBC) (See Fig. 4).

To complete the above thermodynamic description, a kinetic investigation of A_n (n=3,4) was performed in various media at the B3LYP/6-31G(d,p) level of theory for the TS and the B3LYP/6-31+G(d,p) level of theory for the reactants and products. The media considered were a vacuum, benzene, and water. Rate constants were computed at T=298.15 K using the TST/ZCT method.

(ii) ***Height of the potential barrier***

The height of the potential barrier (see Fig. 2 and Fig. 2.s of the ESM) is the activation energy ΔE_a. The activation energy of a reaction (i.e., the parameter that appears in the Arrhenius equation) is directly related to the difference in enthalpy between the TS and the free reactants. The results for these parameters are collected in Table 1, and reveal that the height of the potential barrier increases with solvent polarity. This suggests that increasing the solvent polarity slows down the CPCET mechanism. From site 3, the barrier height increases in the following order: ΔE_a(MBC) < ΔE_a(CAPE) < ΔE_a(BC) < ΔE_a(P3HC). Therefore, the transfer of H_3 from MBC to the radical $^{\bullet}HO_2$ occurs more rapidly than it does from the other molecular systems. From site 4, the barrier height is such that ΔE_a(MBC) < ΔE_a(BC) < ΔE_a(CAPE), while all of these are greater than ΔE_a(P4HC) (see Table 1). Among the molecules studied, P3HC has the highest barrier at site 3, meaning that the hydrogen atom requires more energy to leave its initial site. Moreover, it is also apparent that the barrier heights of CAPE, MBC, and BC at site 4 are higher than those at site 3; therefore the time taken for the H_3 atom to leave its initial site is longer than the time taken for H_4 to leave.

(iii) ***Imaginary frequency and rate constant***

The movement of H_3 (or H_4) between the O_3 (or O_4) of each molecular system studied and the oxygen atom O_A of the radical $^{\bullet}HO_2$ (see Fig. 1) is described by the imaginary frequency ν^*. The absolute value of the imaginary frequency of O–H decreases with solvent polarity (see Table 1), slowing down the motion of the hydrogen atom. We can argue that the movement of the hydrogen atom slows down because it strikes some solvent molecules.

The rate constant highlights the correlation pointed out above. It was computed as shown in TST/ZCT in

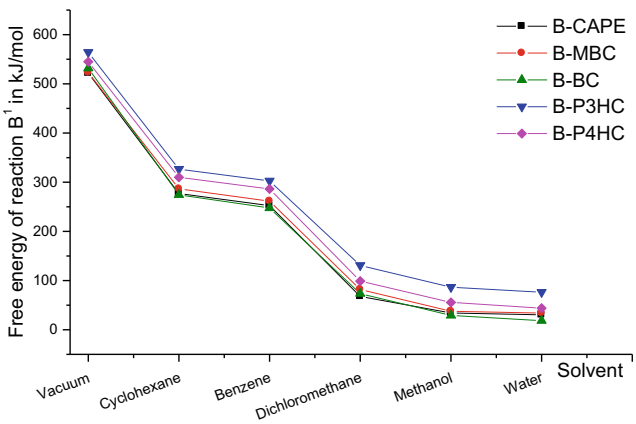

Fig. 5 Free energies of reaction B^1 of B-CAPE, B-P4HC, P3HC, B-MBC, and B-BC in the presence of the radical $^{\bullet}HO_2$ in different media

Table 2 Free energies (in kJ mol^{-1}) of A_n, B^1, $B^2{}_n$, $\Gamma^1{}_n$, $\Gamma^2{}_n$, $\Delta^1{}_n$, and $\Delta^2{}_n$ (n=3,4) reactions involvng the radical $^{\bullet}HO_2$ in different media

Systems	Solvents	$\Delta G(A_3)$	$\Delta G(B^1)$	$\Delta G(B^2{}_3)$	$\Delta G(\Gamma^1{}_3)$	$\Delta G(\Gamma^2{}_3)$	$\Delta G(\Delta^1{}_3)$	$\Delta G(\Delta^2{}_3)$	$\Delta G(A_4)$	$\Delta G(B^2{}_4)$	$\Delta G(\Gamma^1{}_4)$	$\Delta G(\Gamma^2{}_4)$	$\Delta G(\Delta^1{}_4)$	$\Delta G(\Delta^2{}_4)$
B-CAPE	Vacuum	−38.1	522.0	−560.0	734.9	−773.0	1233.2	116.8	−10.8	−532.7	759.6	−770.3	1257.9	117.9
	Cyclohexane	−32.6	277.0	−309.6	457.6	−490.2	377.2	42.5	−18.4	−295.4	472.9	−491.2	392.4	40.4
	Benzene	−31.8	252.3	−284.1	427.2	−458.9	169.0	35.7	−19.2	−271.5	446.3	−465.5	188.1	32.8
	Dichloromethane	−39.1	67.8	−106.9	250.7	−289.9	−336.8	−16.6	−26.8	−94.5	252.6	−279.4	−335.0	−7.4
	Methanol	−24.9	34.1	−59.1	209.3	−234.2	63.6	−16.0	−28.1	−62.2	208.2	−236.3	62.5	−28.1
	Water	−26.0	30.5	−56.5	203.5	−224.2	80.6	−22.6	−29.7	−60.1	194.6	−224.2	71.6	−30.5
	Benzene/SMD	−40.7	269.6	−310.3	367.6	−408.3	167.5	211.1	–	–	–	–	–	–
	Water/SMD	−24.7	−14.7	−10.0	92.4	−117.1	65.2	115.3	–	–	–	–	–	–
B-MBC	Vacuum	−45.7	523.0	−568.7	718.3	−764.0	1232.4	112.9	−18.9	−541.9	766.9	−785.8	1265.2	114.5
	Cyclohexane	−32.3	286.5	−318.7	475.2	−507.5	394.8	40.7	−19.4	−305.9	486.0	−505.4	405.5	37.8
	Benzene	−31.5	261.5	−293.0	449.0	−480.5	190.8	33.9	−20.5	−282.0	459.5	−480.0	201.3	29.9
	Dichloromethane	−33.9	81.9	−115.8	264.7	−298.5	−322.9	−12.6	−18.9	−100.8	260.0	−278.6	−327.9	−0.3
	Methanol	−41.8	37.6	−79.3	212.1	−253.9	66.5	−24.2	−21.5	−59.1	216.6	−238.1	70.9	−12.1
	Water	−33.1	33.9	−67.0	210.0	−243.1	87.1	−26.0	−21.5	−55.4	214.0	−235.5	91.1	−22.3
B-BC	Vacuum	−37.6	531.7	−569.2	741.2	−778.7	1239.5	108.4	−10.8	−542.4	764.0	−774.8	1262.4	109.8
	Cyclohexane	−39.1	274.4	−310.9	459.7	−496.2	379.3	43.9	−19.4	−291.2	479.2	−496.0	398.7	49.9
	Benzene	−38.1	247.6	−285.7	432.4	−470.5	174.2	37.8	−18.9	−266.5	450.5	−469.4	192.3	40.7
	Dichloromethane	−42.0	73.5	−115.5	248.4	−289.9	−339.2	−12.3	−26.8	−100.3	254.7	−281.5	−332.9	−8.1
	Methanol	−41.0	29.2	−70.1	203.7	−244.7	58.1	−22.8	−28.6	−57.8	207.2	−235.8	61.5	−18.9
	Water	−41.5	18.4	−59.9	206.9	−248.4	84.0	−36.8	−28.6	−47.0	196.9	−225.5	74.0	−21.0
B-P3HC	Vacuum	0.0	564.2	−564.2	795.3	−795.3	1293.6	100.6	–	–	–	–	–	–
	Cyclohexane	2.4	326.6	−324.3	515.1	−512.8	434.7	36.5	–	–	–	–	–	–
	Benzene	2.6	302.7	−300.1	487.8	−485.2	229.6	30.5	–	–	–	–	–	–
	Dichloromethane	−4.7	130.8	−135.5	292.2	−297.0	−295.3	−9.5	–	–	–	–	–	–
	Methanol	−7.1	86.6	−93.7	245.8	−252.8	100.1	−20.5	–	–	–	–	–	–
	Water	−5.0	76.2	−81.1	235.5	−240.5	112.6	−20.0	–	–	–	–	–	–
	Vacuum	–	545.1	–	–	–	–	–	−12.3	−557.4	757.2	−769.5	1255.5	132.3
	Cyclohexane	–	310.1	–	–	–	–	–	−9.5	−319.5	476.8	−486.2	396.3	58.6
	Benzene	–	286.2	–	–	–	–	–	−9.5	−295.6	452.6	−462.1	194.4	50.9
B-P4HC	Dichloromethane	–	99.0	–	–	–	–	–	−23.9	−122.9	258.4	−282.2	−329.2	4.2
	Methanol	–	55.7	–	–	–	–	–	−26.3	−81.9	213.5	−239.7	67.8	−8.1
	Water	–	43.9	–	–	–	–	–	−25.7	−69.6	209.8	−235.5	86.9	−8.7

Table 3 Effects of selected polyphenols on DNA damage and toxicity caused by *t*B-OOH in U937 cells [7]

Phenolic compound	IC_{50}[a] (μM)	IC_{50}[b] (μM)
CAPE	0.0203±0.0017	0.0062±0.0005
BC	0.0305±0.0021	0.0130±0.001
MBC	0.0502±0.0038	0.0150±0.001

[a] Concentration of the compound that leads to a 50 % reduction in *t*B-OOH (3 mM)-induced cytotoxicity

[b] Concentration of the compound that leads to a 50 % reduction in *t*B-OOH (200 lM)-induced DNA single-strand breakage

$Å^3\ mol^{-1}\ s^{-1}$. The vibrational and rotational partition functions of the reactants (PhOH and $^{\bullet}HO_2$), those of the products ($PhO^{\bullet}$ and H_2O_2), and finally those of the transition state ($PhO^{\bullet}\cdots H^{\bullet}\cdots{}^{\bullet}HO_2$) were computed in Gaussian 03, but the translational partition function was computed using a homemade Fortran 90 program. The rate constant was found to decrease with solvent (benzene and water) polarity, and the motion of the hydrogen atom slows down (see Table 1). Exceptions are seen in benzene. In this medium, the rate constant is less than that in water for BC, and it slightly increases for CAPE. These results may be useful for studies of the kinetics of the destruction of large biomolecules such as DNA, proteins, etc. by the radical $^{\bullet}HO_2$.

Electron transfer process: ET-PT

The ET-PT mechanism is the reaction labeled B in the "Introduction." In this mechanism the H atom is transferred sequentially: electron transfer (reaction B^1) is followed by proton transfer (reaction B^2). It is worth noting that this mechanism is more favorable in solvent than in vacuum, and in more polar solvents than in less polar ones. The free energies of reactions involving only electron transfer (B^1) are plotted in Fig. 5. From Table 2, we can see that the free energy of reaction B^1 increases in the following order: $B^1(CAPE) < B^1(MBC) < B^1(BC) < B^1(P4HC) < B^1(P3HC)$ in a vacuum and $B^1(CAPE) \sim B^1(BC) < B^1(MBC)$ in solvents, in accord with IC_{50} data (see Table 3). These results are consistent with the earlier explanation regarding the ability of the solvent to separate charged species. They are also consistent with the conclusions drawn based on the ionization potential (IP) and $-E_{HOMO}$ (the energy of the highest occupied molecular orbital) values of the molecules described in [8].

Moreover, from Table 2, $\Delta G(B^1) > \Delta G(B^2{}_n)$ (n=3, 4), regardless of the molecular system studied. This leads us to the following conclusion: the first step of the reaction requires substantial energy to initiate the electron transfer mechanism, while the second step requires only a very small amount of energy.

Proton transfer process: PT-ET/SPLET

The PT-ET mechanism is the reaction denoted Γ in the "Introduction." In this, the H atom is transferred sequentially: proton transfer (reaction Γ^1) is followed by electron transfer (reaction Γ^2). Such a reaction is always unfavorable, especially in a vacuum. This can be explained by noting that the fragmentation of a neutral molecule into a charged species is more difficult to achieve in a vacuum than in a solvent, since the solvent makes the molecule more polar and thus easier to fragment into charged species. In addition, the data for the reaction of $^{\bullet}HO_2$ with H^+ (see Table 4) show that the neutral free radical $^{\bullet}HO_2$ cannot easily interact with a proton, so it is very difficult for PT-ET to happen through this route, especially in a solvent. However, we have still plotted the free energies of reactions involving only proton transfer ($\Gamma^1{}_n$, n=3, 4) in the presence of $^{\bullet}HO_2$ in Fig. 6.s of the ESM. It is clear that the free energy decreases with the increasing dielectric constant. This correlates with the conclusion drawn upon checking the proton affinity (PA) [8] and $\Delta G(\Delta^1{}_n)$ (n=3, 4) data in Table 2. Moreover, $\Delta G(\Gamma^1{}_n) > \Delta G(\Gamma^2{}_n)$ (n=3, 4), regardless of the molecular system studied. Thus, the second step of the reaction requires only a very small amount of energy for electron transfer; in other words, electron transfer occurs very easily.

The data for the reaction of $^{\bullet}HO_2$ with an e^- (see Table 4) show that the neutral free radical $^{\bullet}HO_2$ can easily interact with an electron, so PT-ET can happen through SPLET, as shown in Eq. 4. We are interested in the second equation (Δ^2). Figure 6

Table 4 Free energies (in kJ mol^{-1}) of reactions involving co-reactive species and an abstracted or transferred particle ($H^{\bullet}$, H^+, and e^-), calculated at the B3LYP/6-31++G(d,p) level

Medium	$^{\bullet}HO_2 + H^{\bullet} \rightarrow H_2O_2$	$^{\bullet}HO_2 + H^+ \rightarrow {}^{\bullet}H_2O_2{}^+$	$^{\bullet}HO_2 + e^- \rightarrow {}^{\bullet}HO_2{}^-$	$^{\bullet}O_2{}^- + H^{\bullet} \rightarrow HO_2{}^-$	$^{\bullet}O_2{}^- + H^+ \rightarrow {}^{\bullet}HO_2$
Vacuum	−310.6	−498.3	−96.6	−216.8	−1436.9
Cyclohexane	−295.8	80.5	−252.5	−206.3	−518.7
Benzene	−296.3	258.2	−254.5	−207.9	−308.6
Dichloromethane	−301.9	587.6	−33.5	−223.6	234.7
Methanol	−303.7	145.7	−313.2	−229.7	−157.0
Water	−351.7	122.9	−303.7	−278.9	−169.0

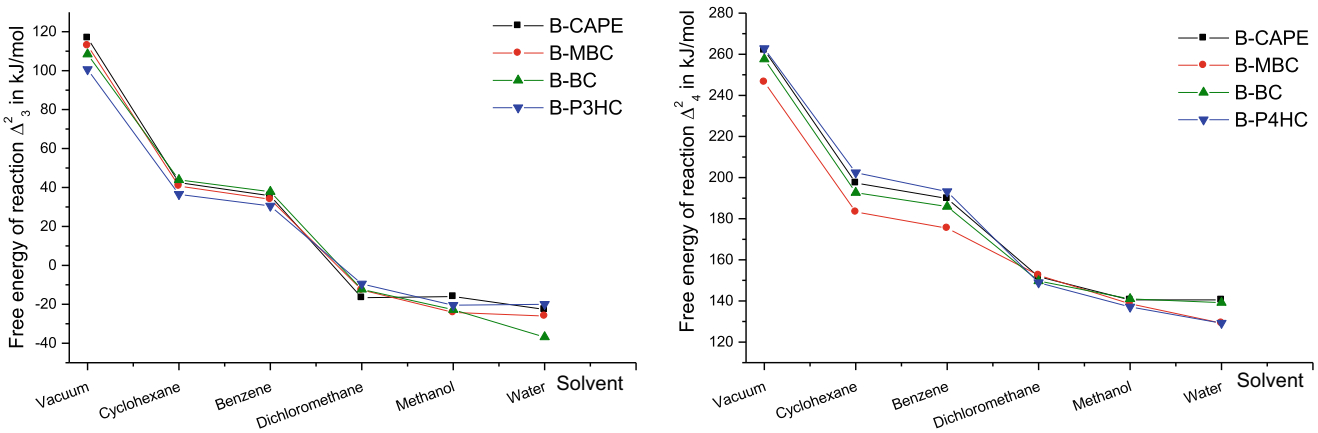

Fig. 6 Free energies of the reactions Δ^2_3 (*left*) and Δ^2_4 (*right*) for B-CAPE, B-P4HC, P3HC, B-MBC, and B-BC with the radical $^{\bullet}HO_2$ in different media

and Table 2 display the relevant results, which suggest that it is more favorable in solvent than in a vacuum, and the more polar the solvent, the more favorable the mechanism. This is because the solvents, especially polar solvents, have the ability to separate charged species; the anion PhO^- is more stable in a polar environment, facilitating electron transfer. Furthermore, it is easier for P3HC in a vacuum or a nonpolar solvent to scavenge $^{\bullet}HO_2$ than it is for the other systems studied here to do so. Therefore, BC and MBC are more active in a polar solvent. The results in Table 2 show that this

Table 5 Free energies (in kJ mol^{-1}) of A_3, A_4, Γ^1_3, Γ^2_3, Γ^1_4, and Γ^2_4 reactions involving the radical $^{\bullet}O_2^-$ in different media

System	Solvent	$\Delta G(A_3)$	$\Delta G(\Gamma^1_3)$	$\Delta G(\Gamma^2_3)$	$\Delta G(A_4)$	$\Delta G(\Gamma^1_4)$	$\Delta G(\Gamma^2_4)$
B-CAPE	Vacuum	55.7	−203.8	259.4	83.0	−179.1	262.0
	Cyclohexane	57.0	−141.5	198.5	71.2	−126.3	197.4
	Benzene	56.7	−139.7	196.4	69.3	−120.5	189.8
	Dichloromethane	39.1	−102.1	141.3	51.5	−100.3	151.8
	Methanol	49.1	−93.5	142.6	46.0	−94.5	140.5
	Water	46.7	−88.5	135.2	43.1	−97.4	140.5
	Vacuum/CBS	87.4	−68.5	156.0	–	–	–
	Benzene/SMD	49.1	−162.0	211.1	–	–	–
	Water/SMD	37.6	−77.7	115.3	–	–	–
B-MBC	Vacuum	48.1	−204.5	268.3	74.8	−171.7	246.5
	Cyclohexane	57.2	−123.9	181.2	70.1	−113.2	183.3
	Benzene	57.0	−117.9	174.9	68.0	−107.4	175.4
	Dichloromethane	44.4	−88.2	132.6	59.3	−93.2	152.5
	Methanol	32.3	−90.6	122.9	52.5	−86.1	138.6
	Water	39.7	−81.9	121.6	51.2	−78.0	129.2
B-BC	Vacuum	56.2	−197.5	253.6	83.0	−174.6	257.6
	Cyclohexane	53.0	−139.4	192.5	72.7	−120.0	192.7
	Benzene	50.4	−134.4	184.8	69.6	−116.3	185.9
	Dichloromethane	36.2	−104.5	140.7	51.5	−98.2	149.7
	Methanol	33.1	−99.0	132.1	45.4	−95.6	141.0
	Water	31.2	−85.1	116.3	44.1	−95.1	139.2
	Vacuum	93.7	−143.4	237.1	81.4	−181.4	262.8
	Cyclohexane	92.0	−84.0	175.9	80.1	−122.4	202.4
B-P3HC	Benzene	91.1	−79.0	170.1	79.0	−114.2	193.2
B-P4HC	Dichloromethane	73.5	−60.7	134.2	54.4	−94.5	148.9
	Methanol	67.0	−57.0	123.9	47.8	−89.3	137.1
	Water	67.7	−56.5	124.2	47.0	−82.2	129.2

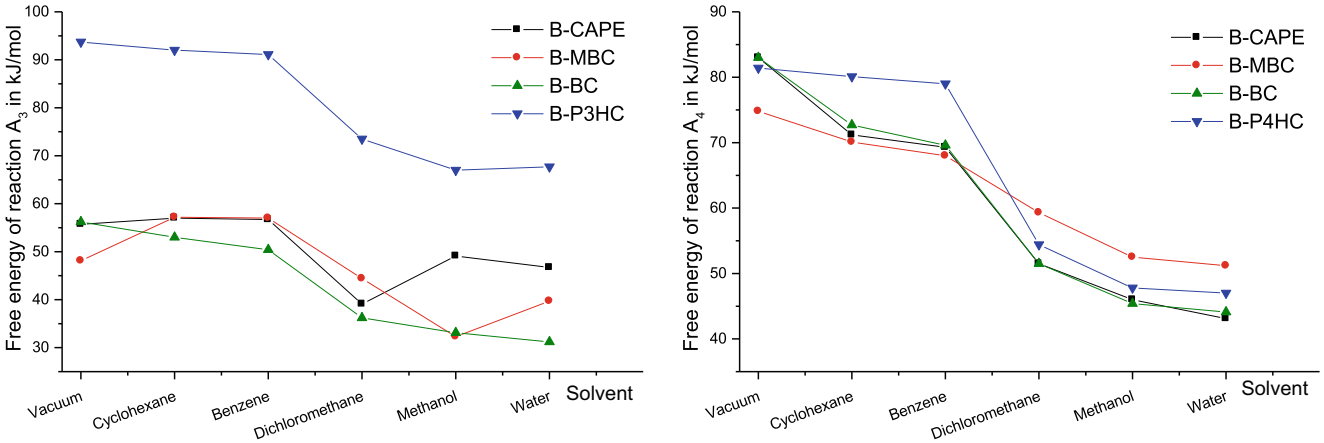

Fig. 7 Free energies of the reactions A_3 (*left*) and A_4 (*right*) of B-CAPE, B-P4HC, P3HC, B-MBC, and B-BC in the presence of radical $^{\bullet}O_2^-$ in different media

kind of scavenging at site 4 is facilitated in a vacuum, as well as in polar solvents for CAPE and BC. The table shows that $\Delta G(\Gamma^1{}_n) > \Delta G(\Delta^2{}_n)$ (n=3, 4), so the preferred mechanism is SPLET, in agreement with the results from [52].

Scavenging of $^{\bullet}O_2^-$ by CAPE and its derivatives

This section focuses on reactions involving polyphenols (the family of molecules chosen in this study) and superoxide $^{\bullet}O_2^-$. Since this radical is ionic, the only possible reactions are CPCET and PT-ET (or simply proton transfer, PT) because the ionic radicals have the same charge as an electron (i.e., repulsion occurs). Figure 2 presents the stationary states for H-atom transfer process in the reaction involving CAPE and $^{\bullet}O_2^-$. There is no barrier to overcome; the reaction is barrierless.

Atom transfer process: CPCET

The data for the reaction of $^{\bullet}O_2^-$ with $H^{\bullet}$ (see Table 4) show that the ionic free radical $^{\bullet}O_2^-$ can interact with one H atom, as predicted by Dhaouadi et al. [22]. It is therefore obvious that CPCET can occur in any environment. Table 5 displays the results for the free energies of the reactions A_n, where n=3, 4 denotes the position of −OH on the ring in each molecule studied. Figure 7 displays the free energy values in different media and the corresponding reported numerical values from Table 5, and shows that $\Delta G(A_3) < \Delta G(A_4)$ in a vacuum as well as in the solvents. Therefore, site 3 remains susceptible to radical attack, as discussed above. The results also reveal that the free energy of reaction A_3 in a vacuum increases in the order A_3(MBC) < A_3(CAPE) < A_3(BC) < A_3(P3HC), which agrees with the order established from the BDE_3 data [8] for the case involving $^{\bullet}HO_2$ discussed above. In solvents, BC has the lowest values of $\Delta G(A_3)$, so its antioxidant capacity is greater than those of the other systems among this family of molecules. At site 4, we have A_4(MBC) < A_4(P4HC) < A_4(CAPE) ~ A_4(BC) in a vacuum, which confirms that MBC is the most active antioxidant, whereas in strongly polar solvents (dichloromethane, methanol, and water) A_4(CAPE) < A_4(BC) < A_4(P4HC) < A_4(MBC). The results obtained in the presence of the neutral radical $^{\bullet}HO_2$ agree with those gained in the presence of the ionic radical $^{\bullet}O_2^-$.

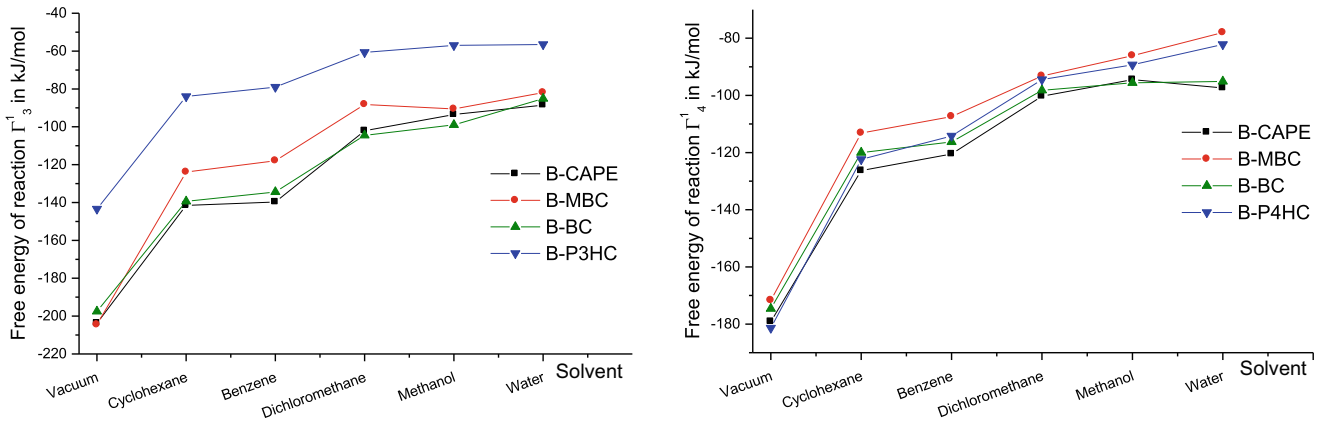

Fig. 8 Free energies of the reactions $\Gamma^1{}_3$ (*left*) and $\Gamma^1{}_4$ (*right*) of B-CAPE, B-P4HC, P3HC, B-MBC, and B-BC in the presence of the radical $^{\bullet}O_2^-$ in different media

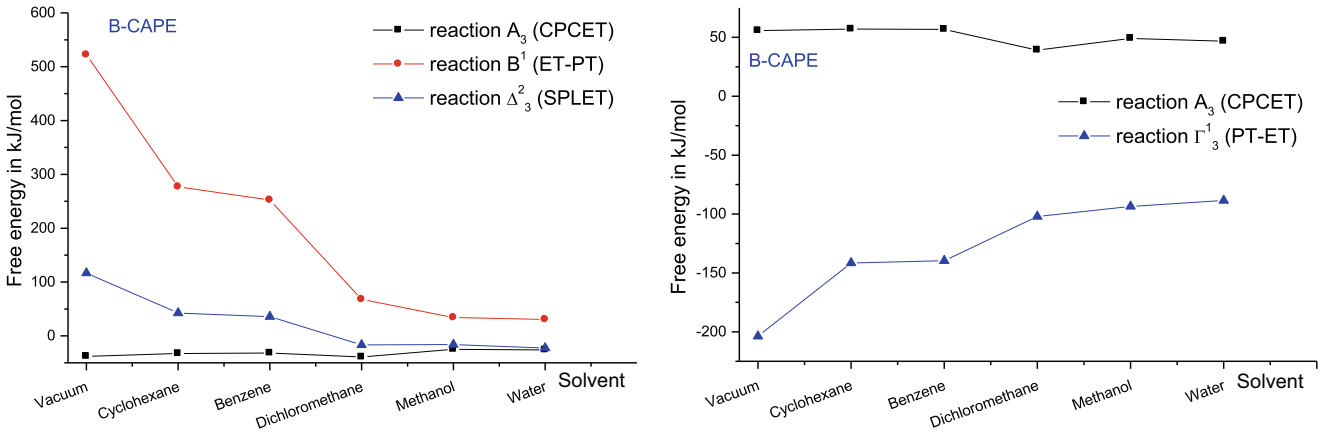

Fig. 9 Free energies of the reactions A_n, B^1_n, and Γ^1 (n=3,4) of B-CAPE in the presence of the radical $^{\bullet}HO_2$ (*right*) and the radical $^{\bullet}O_2^-$ (*left*) in different media

Proton transfer process: PT-ET

This sequential process is always favorable in any environment; the data for the reaction of $^{\bullet}O_2^-$ with H^+ (see Table 4) show that the ionic free radical $^{\bullet}O_2^-$ easily interacts with a proton, as predicted by Dhaouadi et al. [22], so it is obvious that PT-ET can happen in any environment. We have plotted the free energies of reactions involving only proton transfer (Γ^1_n, n=3,4) in the presence of $^{\bullet}O_2^-$ in Fig. 8. It is clear that free energy increases with increasing dielectric constant. Therefore, this process is more favorable in a vacuum.

In addition, $\Delta G(\Gamma^1_n) < \Delta G(\Gamma^2_n)$ (n=3, 4), regardless of the molecular system studied. Thus, the second step of the reaction requires more energy for electron transfer (ET); in other words, it is very difficult for an electron to be transferred in the second step. This means that, in reality, only proton transfer (PT) occurs in this case.

Moreover, as concluded above, site 3 remains the most likely site to engage in free-radical scavenging (since $\Delta G(\Gamma^1_3) > \Delta G(\Gamma^1_4)$). Furthermore, at site 3 in nonpolar solvents and at site 4 in any environment, we obtained the following order of free energy: Γ^1_n(CAPE) < Γ^1_n(BC) < Γ^1_n(MBC) (n=3, 4); this is similar to the conclusion drawn based on IC_{50} data (see Table 3).

The preferred mechanism

To evaluate the preferred mechanism of the molecular system studied in the presence of the neutral free radical $^{\bullet}HO_2$ and in the presence of the ionic free radical $^{\bullet}O_2^-$, we plotted the free-energy values of reactions A, B^1, and Δ^2 from site 3 on the right hand side of Fig. 9 (see also Fig. 9.s of the ESM) and the free-energy values of reactions A and Γ^1 from site 3 on the left hand side of the same figure (see Fig. 9.s of the ESM). The $\Delta G(A_3)$ values were found to be very low whatever the environment and the molecular system studied in the presence of the radical $^{\bullet}HO_2$. It is therefore clear that the preferred mechanism is CPCET. However, the SPLET data is close to the CPCET data in polar solvents, so SPLET could occur rather than the CPCET mechanism, meaning that these pathways are competitive in polar environments. Nevertheless, the $\Delta G(\Gamma^1_3)$ values are very low regardless of the environment and molecular system studied in the presence of the radical $^{\bullet}O_2^-$, so the preferred mechanism in this case is PT-ET. Tables 2 and 5 suggest that the same conclusions can be drawn for site 4.

The above discussions allow us to assert that whatever the environment, CPCET is the preferred mechanism when phenolic acids are in the presence of neutral radicals, even though the two pathways are competitive in polar solvents. Recently, Bobrowski et al. [53] came to the same conclusion regarding electron and proton transfer, although they studied the generation of reactive oxygen species from triplet oxygen and semiquinone radicals. In contrast, PT-ET is the preferred mechanism when phenolic acids are in the presence of ionic radicals.

Conclusions

In quantum chemical calculations that were presented briefly here, the B3LYP/6-31G(d,p) level of DFT was used for optimizations and then the B3LYP/6-31+G(d,p) level was used for frequency calculations. The CPCM was used to study the effect of the solvent. Our calculations showed that, in the presence of co-reactive species, the CPCET mechanism dominates over the HHAT mechanism. In the presence of neutral free radicals, CPCET is the preferred mechanism whatever the environment, but the CPCET and SPLET processes remain competitive in polar solvents. In the presence of ionic free radicals, PT-ET is the preferred mechanism. From thermodynamic investigations, we concluded that site 3 is more susceptible to radical attack than site 4. In addition, in a vacuum, the antioxidant activity of MBC appears to be greater than

those of the other systems in the family of molecules studied, while CAPE presents the highest antioxidant activity according to IC_{50} data. This behavior was also seen in strongly polar solvents in this study. The free energies $\Delta G(B^1)$ and $\Delta G(\Gamma^1{}_n)$ only contradict the IC_{50} data in a vacuum, where MBC was observed to have the highest antioxidant activity. Another feature is that there are many changes in $\Delta G(A_n)$ when we move from a vacuum to solvents; however, $\Delta G(B^1)$ and $\Delta G(\Delta^2{}_n)$ as well as IP and PA_n [8] and $\Delta G(\Delta^1{}_n)$ (n=3, 4) show that solvents increase the antioxidant capacities of the PhAs. From a kinetics viewpoint, the higher the solvent's polarity, the slower the CPCET mechanism.

Acknowledgments The authors are grateful to the Abdus Salam International Centre For Theoretical Physics for their financial support of this work through the Office of External Activities - NET 45 Poject.

References

1. Soobrattee MA, Neergheen VS, Luximon-Ramma A, Aruoma OI, Bahorun T (2005) Mutat Res 579:200
2. Nsangou M, Dhaouadi Z, Jaïdane N, Ben Lakhdar Z (2008) J Mol Struct THEOCHEM 850:135 (and references therein)
3. Nsangou M, Fifen JJ, Dhaouadi Z, Lahmar S (2008) J Mol Struct THEOCHEM 862:53 (and references therein)
4. Rajan P, Vedernikova I, Cos P, Vanden Berghe D, Augustyns K, Haemers A (2001) Bioorg Med Chem Lett 11:215
5. Chen JH, Ho C-T (1997) J Agric Food Chem 45:2374
6. Son S, Lobrowsky EB, Lewis BA (2001) Chem Pharm Bull 49:236
7. Sestili P, Diamantini G, Bedini A, Ceroni L, Tommasini I, Tarziq G, Cantoni O (2002) Biochem J 364:121
8. Holtomo O, Nsangou M, Fifen JJ, Motapon O (2013) J Chem Chem Eng 7:910
9. Fesen MR, Kohn KR, Leteurtre F, Pommier Y (1993) Proc Natl Acad Sci USA 90:2399
10. Kujumgiev A, Bankova V, Ignatova A, Popov S (1993) Pharmazie 48: 785
11. Mirzoeva OK, Kalder PC (1996) Prostaglandins Leucot Essent Fat Acids 55:441
12. Orban Z, Mitsiades N, Burke TR, Tsokos M Jr, Chrousos GP (2000) Neuro Immuno Modulation 7:99
13. Lefkovits I, Su Z–Z, Fisher PB, Grunberger D (1997) Int J Oncol 11: 59
14. Sud'ina GF, Mirzoeva OK, Pushkharaeva MK, Korshunova GA, Shubatyan NV, Varfolomeev SD (1993) FEBS Lett 329:21
15. Fiorucci S, Golebiowski J, Bass DC, Antonczak S (2007) J Agric Food Chem 55:903
16. Alberto ME, Russo N, Grand A, Galano A (2013) Phys Chem Chem Phys 15:4642
17. Meo FD, Lemaur V, Cornil J, Lazzaroni R, Duroux JL, Olivier Y, Trouillas P (2013) J Phys Chem A 117:2082
18. Mayer JM (2004) Annu Rev Phys Chem 55:363
19. Mayer JM, Hrovat DA, Thomas JL, Borden WT (2002) J Am Chem Soc 124:11142
20. Mayer JM, Rhile IJ (2004) Biochim Biophys Acta 1655:51
21. Dempsey JL, Winkler JR, Gray HB (2010) Chem Rev 110:7024
22. Dhaouadi Z, Nsangou M, Garrab N, Anour EH, Marakchi K, Lahmar S (2009) J Mol Struct THEOCHEM 904:35
23. Zhang HY, Wang L-F (2003) J Phys Chem A 107:11258
24. Fifen JJ, Nsangou M, Dhaouadi Z, Motapon O, Jaïdane N (2011) Comput Theor Chem 966:232
25. Fifen JJ, Nsangou M, Dhaouadi Z, Motapon O, Lahmar S (2009) J Mol Struct THEOCHEM 901:49
26. Glod BK, Kowalski C (2004) Pol J Food Nutr Sci 13(54):23
27. Michelson AM, McCord JM, Fridovich I (1977) Superoxide and superoxide dismutases. Academic, London
28. Liochev SI, Fridovich I (2001) Arch Biochem Biophys 388:281
29. Nagaoka S, Kuranaka A, Tsuboi H, Hagashima U, Kumai K (1992) J Phys Chem 96:2754
30. Wright JS, Johnson ER, Dilabio GA (2001) J Am Chem Soc 123: 1173
31. Frisch MJ, Trucks GW, Schlegel HB, Scuseria GE, Robb MA, Cheeseman JR, Montgomery JA Jr, Vreven T, Kudin KN, Burant JC, Millam JM, Iyengar SS, Tomasi J, Barone V, Mennucci B, Cossi M, Scalmani G, Rega N, Petersson GA, Nakatsuji H, Hada M, Ehara M, Toyota K, Fukuda R, Hasegawa J, Ishida M, Nakajima T, Honda Y, Kitao O, Nakai H, Klene M, Li X, Knox JE, Hratchian HP, Cross JB, Adamo C, Jaramillo J, Gomperts R, Stratmann RE, Yazyev O, Austin AJ, Cammi R, Pomelli C, Ochterski JW, Ayala PY, Morokuma K, Voth GA, Salvador P, Dannenberg JJ, Zakrzewski VG, Dapprich S, Daniels AD, Strain MC, Farkas O, Malick DK, Rabuck AD, Raghavachari K, Foresman JB, Ortiz JV, Cui Q, Baboul AG, Clifford S, Cioslowski J, Stefanov BB, Liu G, Liashenko A, Piskorz P, Komaromi I, Martin RL, Fox DJ, Keith T, Al-Laham MA, Peng CY, Nanayakkara A, Challacombe M, Gill PMW, Johnson B, Chen W, Wong MW, Gonzalez C, Pople JA (2003) Gaussian 03, revision B.05. Gaussian, Inc., Pittsburgh
32. Becke AD (1998) Phys Rev A 38:3098
33. Lee C, Yang W, Parr RG (1988) Phys Rev B 37:785
34. Ditchfield R, Hehre WJ, Pople JA (1971) J Chem Phys 54:724
35. Hehre WJ, Ditchfield R, Pople JA (1972) J Chem Phys 56: 2257
36. Hariharan PC, Pople JA (1974) Mol Phys 27:209
37. Francl MM, Pietro WJ, Hehre WJ, Binkley JS, DeFrees DJ, Pople JA, Gordon MS (1982) J Chem Phys 77:3654
38. Rassolov VA, Pople JA, Ratner MA, Windus TL (1998) J Chem Phys 109:1223
39. Rassolov VA, Ratner MA, Pople JA, Redfern PC, Curtiss LA (2001) J Comput Chem 22:976
40. Clark T, Chandrasekhar J, Spitznagel GW, Schleyer PVR (1983) J Comput Chem 4:294
41. Marenich AV, Cramer CJ, Truhlar DG (2009) J Phys Chem B 113(18):6378
42. Rayne S, Forest K (2010) Nat Proc. doi:10.1038/npre.2010.4864.1
43. Jurečka P, Šponer J, Černý J, Hobza P (2006) Phys Chem Chem Phys 8:1985
44. Truong TN, Truhlar DG (1990) J Chem Phys 93:1761
45. Duncan WT, Bell RL, Truong TN (1998) J Comput Chem 19:1039
46. Buchowiecki M, Vanicek J (2010) J Chem Phys 132:194106
47. Truhlar DG, Kuppermann A (1971) J Am Chem Soc 93:1840
48. Truhlar DG, Kuppermann A (1971) Chem Phys Lett 9:269
49. Eckart C (1930) Phys Rev 35:1303
50. Skodje RT, Truhlar DG (1981) J Phys Chem 85:624
51. Wigner E (1932) Z Phys Chem B 19:203
52. Rimarcik J, Lukes V, Klein E; Ilcin M (2010) J Mol Struct THEOCHEM 952:25
53. Bobrowski M, Liwo A, Hirao K (2007) J Phys Chem B 111: 3543